Numerical Simulation of Rocket Engine Internal Flows

Project Representative
Masao Furukawa Institute of Space Technology and Aeronautics, Japan Aerospace Exploration Agency

Authors
Taro Shimizu Institute of Space Technology and Aeronautics, Japan Aerospace Exploration Agency
Nobuhiro Yamanishi Institute of Space Technology and Aeronautics, Japan Aerospace Exploration Agency
Chisachi Kato Institute of Industrial Science, The University of Tokyo
Nobuhide Kasagi Department of Mechanical Engineering, The University of Tokyo

This year, one of our main focuses was on combustion gas leaking from the nozzle wall of the solid rocket booster, which was considered the primary cause of the trouble of Japanese H-2A launch vehicle No. 6. In order to prove the trouble scenario, we performed numerical simulation to understand the temporal behavior of the combustion gas leaking into the rear adapter. From the numerical results, we can calculate the heat flux of specified locations where the real values are known. The agreement between calculated and real heat fluxes is fairly good, verifying that the trouble is caused by combustion gas leaking from the hole in the nozzle wall created by erosion. Large Eddy Simulation (LES) code was developed in order to compute accurately the cavitating flow in turbomachinery. The code was applied to compute non-cavitating flow in a multistage centrifugal pump to validate the accuracy of computed pressure fluctuation. Cavitation model was validated in the computation of cavitating flow around a two dimensional foil (NACA0015). In both cases good agreements were obtained. Finally, Direct numerical simulation of a turbulent channel flow at $Re_\tau = 2320$ was performed in order to improve turbulence models to be applicable in high Reynolds number wall-turbulence. The visualized flow field and the turbulent statistics suggest that the streaky structures, of which spanwise spacing is about 100 wall units, exist only near the wall ($y^+ < 30$), while the large-scale structures extend from the center of the channel to the near-wall region ($y^+ \sim 30$). Therefore, the near-wall turbulence depends not only on the near-wall fine-scale structures, but also on the large-scale structures.

Keywords: H-2A rocket, SRB-A, rocket turbopump, large eddy simulation, wall turbulence, direct numerical simulation

Understanding the physics of the internal flow of a rocket engine is essential for developing a highly reliable space launch vehicle. Until recently, the development of Japanese rockets was largely based on trial and error, i.e. an iterative cycle of trial design and experimental verification. Recent progress in computational fluid dynamics has changed this approach, as numerical simulation is now playing a major role in the development of rockets and rocket engines built today. This year, one of our main focuses was on combustion gas leaking from the nozzle wall, which was considered the primary cause of the trouble of Japanese H-2A launch vehicle No. 6. Japanese H-2A launch vehicle No. 6 was launched in November 2003. However, the system for separating one of the solid rocket booster (SRB-A) from the body of the main rocket would not work, causing the mission to be aborted. The primary cause of the trouble is assumed to be as follows. Erosion caused by the combustion gas inside the nozzle melted the nozzle wall made of composite material and made small holes in the nozzle wall. Hot gas then leaked into the rear adapter that shields the electric instruments from the open air. Finally, a fuse in the separation mechanism for SRB-A was exposed to the hot gas and melted. In order to prove the above trouble scenario, we performed numerical simulation to understand the temporal behavior of the hot gas inside the rear adapter. The unstructured grid system that has been used so far was applied to reproduce the actual shape of the rear adapter, including the electric instruments. A numerical method of solving the Navier-Stokes equations on the hybrid grid was developed using a finite-volume cell vertex scheme and the LU-SGS implicit time integration algorithm[1, 2]. The numerical simulation was performed to determine the position and size of the hole on the nozzle wall. Figure 1 depicts the schematic of SRB-A. The position of the hole is assumed to be slightly downstream of the nozzle throat. The rear adaptor contains many electrical instruments. Figure 2 illustrates the temporal behavior of the hot gas inside the rear adapter. The left-hand side represents the iso-surface at which the mass fraction of the hot gas equals 0.05. The right-hand side represents the wall temperature of the rear adapter. The leaking gas flows through the narrow path between the nozzle and rear

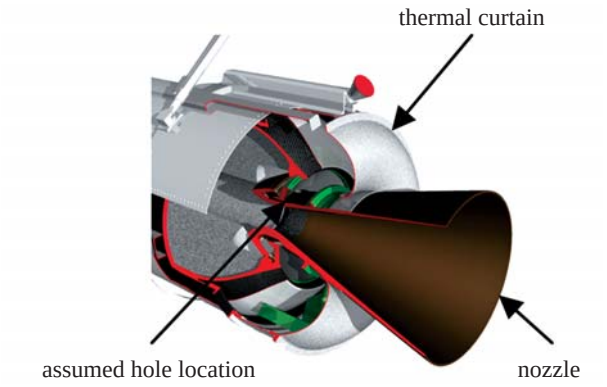

Fig. 1 Schematic of SRB-A (solid rocket booster).

adapter, and then breaks against the thermal curtain. After that, the hot gas slowly spread toward the opposite phase. From the numerical results, we can calculate the heat flux of specified locations where the real values are known. The agreement between calculated and real heat fluxes is fairly good, verifying that the trouble is caused by combustion gas leaking from a hole in the nozzle wall created by erosion. Finally, the propellant shape and the nozzle contour that cause the high heat flux, the thickness of the nozzle wall and the location of the fuse were reconsidered or improved, and a newly designed SRB-A was tested on the ground. In February

a) 1ms

b) 20ms

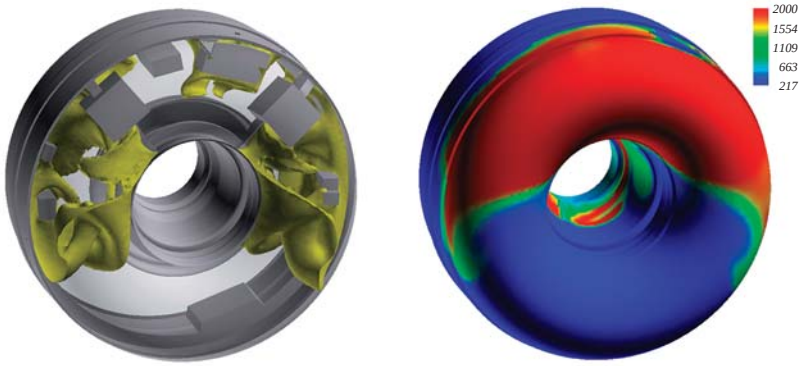

c) 100ms

Fig. 2 Temporal behavior of the combustion gas leaking.
Iso-surface at which the mass fraction of the hot gas equals 0.05 (left-hand side) and wall temperature of the rear adapter (right-hand side).

2005, H-2A launch vehicle No. 7 had a successful launch with an improved SRB-A.

Computational Fluid Dynamics (CFD) is becoming an important tool for design and development of reliable turbomachinery. Not only the steady predictions such as the characteristic curve but also the predictions for unsteady phenomena such as pressure fluctuation are important issues. In addition, it is also the key issue to predict accurately the effect of cavitation generated in turbomachinery. Many researches have been done for the computations of the internal flow of turbomachinery[3, 4]. Most of these computations are based on Reynolds Averaged Navier-Stokes Simulation (RANS). Since RANS is essentially based on time-averaging concept and models dynamics of eddies, we cannot expect an accurate prediction of unsteady phenomena from RANS. On the other hand a large eddy simulation (LES) directly deals with dynamics of eddies resolved by the computational grids, and it has potential to compute unsteady flow more accurately than RANS. Moreover LES seems to be suitable for the computations of cavitating flow because generation and disappearance of cavitation depend on the unsteady pressure field. In this study, we develop LES code to compute accurately unsteady flow including cavitation in turbomachinery. In this fiscal year, we performed LES for the non-cavitating flow in a multistage centrifugal pump in order to validate the accuracy of pressure fluctuations. We also performed preliminary tests for cavitating flow around a two dimensional hydrofoil (NACA0015). Computed pressure fluctuations in the pump and computed fluid force acting on the foil were respectively compared with the measured data.

The code developed in this study is parallel LES code, in which Dynamic Smagorinsky model is implemented as Sub-Grid Scale (SGS) model. This code is based on finite element method with hexahedral elements and has the second order accuracy in time and space[5]. By the multi-frame of reference function based on an overset method, it is possible to compute rotor-stator interaction[6]. For computation of cavitating flow, we implemented the cavitation model proposed by Okita, et al[7]. This models the generation and disappearance of cavitation according to the relation between the vapor pressure and fluid static pressure.

We performed LES of the non-cavitating internal flow of a multistage centrifugal pump[8]. Test pump investigated in this case is a 5-stage centrifugal pump. Each stage is composed of a shrouded impeller, a vaned diffuser and a vaned return channel. The specific speed of the pump is about 200 [rpm, m^3/min, m]. The total number of the finite elements used for LES is about 37 millions among which approximately 0.3 million elements are dedicated to one blade passage. The LES was done at two operation points: the designed point and 50% off-designed point. For the inlet boundary condition, uniform velocities were given according to the flow rate. We applied the non-slip condition for the wall boundary, and the traction free condition for the outlet boundary. We used 32 nodes (256 CPUs) of the Earth Simulator. The sustained performance was about 180 GFLOPS that is about 7% of the peak performance. Figure 3 shows the distributions of the instantaneous pressure fluctuations on the surface of the pump. The pressure fluctuation is defined as the difference between the instantaneous and time averaged static pressure normalized by the density and measured total head at the designed point. The fluctuation at off-designed point is higher than those at designed point. Figure 4 shows the comparisons of measured and computed pressure fluctuations at the 3rd stage diffuser. The pressure fluctuations are presented with the amplitude in terms of their frequency spectra. The frequency is normalized to the Strouhal number by the rotational speed and the number of impeller blades. In spectrum distributions, good agreements are obtained not only at the blade passing frequency (BPF) but also for the base level that reflects the energy cascade among vortices. Moreover, we could capture the trend that the base level of the pressure fluctuations at the off-designed point is higher than one at the designed point.

As the next step, we performed primitive tests for cavita-

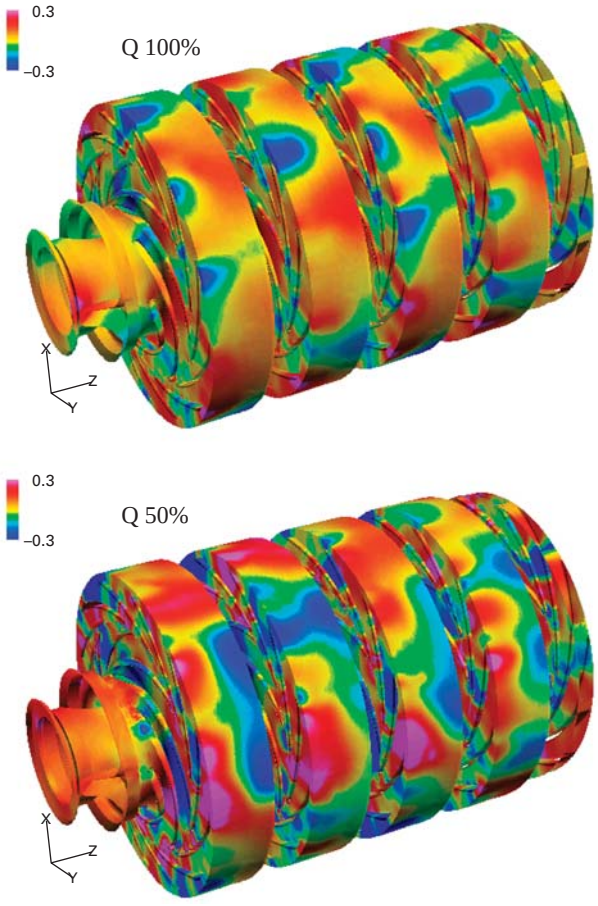

Fig. 3 Distributions of the instantaneous pressure fluctuations on the surface of the multi-stage centrifugal pump.
(top: designed point, bottom: off-designed point 50%)

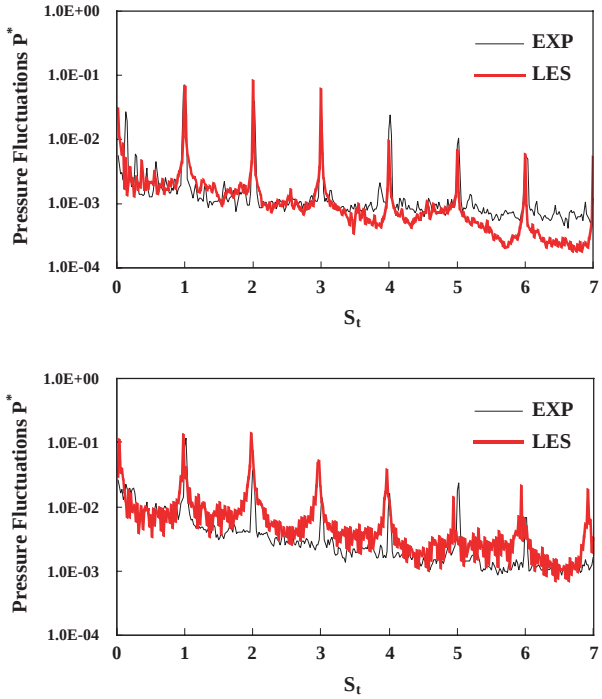

Fig. 4 Comparisons of the pressure fluctuation at the 3rd diffuser. (top: designed point, bottom: off-designed point 50%)

tion model [9]. We applied our code to cavitating flow around a two dimensional hydrofoil (NACA0015) and compared the computed drag and lift coefficients with measured ones[10]. Reynolds number based on the mainstream velocity and chord length is 1.2×10^6 and the attack angle is 8 degree. The total number of the finite elements used for LES is about 1.2 million. Non-slip condition was applied to the hydrofoil surface and side wall. Note that turbulent boundary layer (TBL) on the hydrofoil surface is resolved but grid resolution near the side wall is not fine enough to resolve TBL in this computation. We used 8 nodes (64 CPUs) of the Earth Simulator. The sustained performance was about 50 GFLOPS that is about 10% of the peak performance. Figure 5 shows the distributions of liquid fraction on the mid-span plane. Larger cavitation region with lower cavitation number σ indicates that we can compute cavitating flow at least in a qualitative sense. Figure 6 shows comparisons of the drag and lift coefficients. We were able to obtain good agreements except for the brake down point (σ = 1.15). We think the reason for the discrepancy is the underestimation of eddy viscosity. The improvement of fluid force prediction is the next problem to be overcome. We will take the relationship between the cavitation and eddy viscosity into account.

Finally, some fundamental characteristics of a turbulent channel flow at Re_τ = 2320 are studied by means of direct numerical simulation (DNS). Our aim is to accumulate the essential knowledge on high-Reynolds number wall-turbulence, which can be used for improvement of turbulence models, such as subgrid-scale model in above-mentioned LES. It is well known that near-wall streamwise vortices

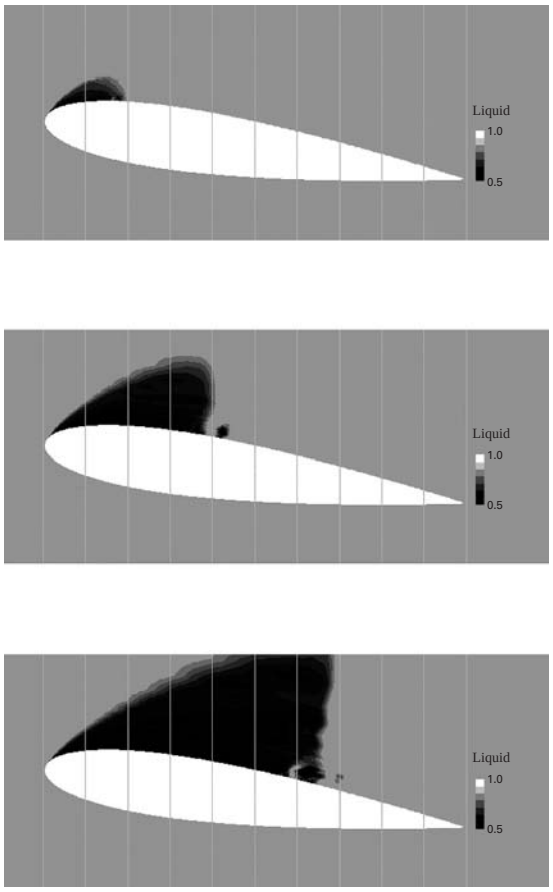

Fig. 5 Instantaneous field of liquid fraction at the mid-span plane in cavitating flow around NACA0015. (top σ = 1.6, middle σ = 1.15, bottom σ = 0.9)

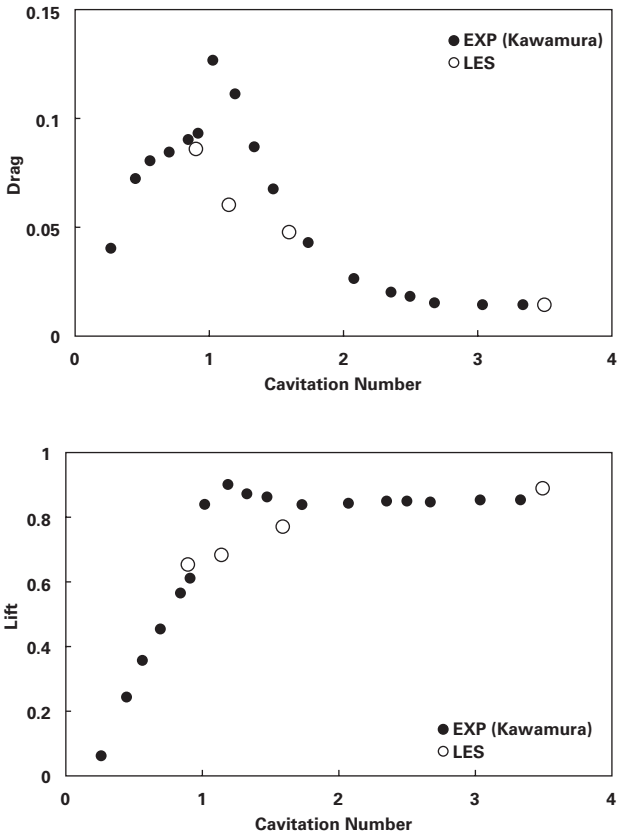

Fig. 6 Comparison of fluid forces on NACA0015. (top: drag, bottom: lift)

play an important role in the transport mechanism in wall turbulence, at least, at low Reynolds numbers[11]. On the other hand, the fundamental characteristics of the large-scale outer-layer structures at higher Reynolds numbers still remain unresolved. In the present study, DNS of turbulent channel flow at a Reynolds number of $Re_\tau = 2320$, which can be reached by the most powerful supercomputer system at this moment, is carried out to examine the flow statistics at high Reynolds numbers and the effect of the large-scale structures on the near-wall turbulence. The numerical method used in the present study is almost the same as that of Kim *et al.*[12]; a pseudo-spectral method with Fourier series is employed in the streamwise (x) and spanwise (z) directions, while a Chebyshev polynomial expansion is used in the wall-normal (y) direction. The number of the total grid points is about 16 billions, and the effective computational speed is about 5.5 TFLOPS by using 2048 CPUs and 4 TB main memory on the Earth Simulator. See Ref. 13 for the numerical procedures and parameters in detail. Hereafter, u, v, and w denote the velocity components in the x-, y-, and z-directions, respectively. Superscript ($^+$) represents quantities non-dimensionalized with u_τ and ν.

Figure 7 shows the ($x - z$) plane views of instantaneous near-wall flow fields at $y^+ \sim 11$, in which contours of the streamwise velocity fluctuation u' are visualized. The area of the upper figure is the whole computational domain. It is found that there are some large-scale streaky structures near the wall, of which spanwise scale is estimated at about 1.2 δ based on the pre-multiplied energy spectra (not shown here), where δ is the channel half width. The lower figure is an enlarged view of the upper one. The fine-scale streaky structures with spanwise scale of about 100 wall units observed here are similar to those in low Reynolds number flows. It is clearly recognized that the fine-scale streaky structures are mixed with the large-scale ones, indicating that the large-scale structures affect the near-wall coherent structures. Figure 8 shows the ($y - z$) cross-stream planes of an instantaneous flow field, in which contours of the streamwise velocity fluctuation u' are visualized. The area of the upper figure is the whole computational domain. It is found that the large-scale structures exist from the center of the channel to the near-wall region. The spanwise scale at any y-location is roughly estimated at $\sim \delta$ based on the pre-multiplied energy spectra (not shown here). The lower figure is an enlarged view of the upper one. The streaky structures, of which spanwise spacing is about 100 ν / u_τ, exist only near the wall ($y^+ < 30$), while the large-scale structures exist from the central region of the channel to the region very near the wall ($y^+ \sim 30$).

Bibliographies

1) Tohoku University Aerodynamic Simulation Code (TAS).
2) M. Kodera, T. Sunami, and K. Nakahashi, "Numerical Analysis of SCRAMJET Combusting Flows by Unstructured Hybrid Grid Method," AIAA 00-0886, Jan. 2000.
3) C. E. Brennen, *Hydrodynamics of Pumps*, Concept ETI Inc. and Oxford University Press, 1994.
4) R. P. Dring, H. D. Joslyn, L. W. Hardin, and J. H. Wagner, "Turbine Rotor-Stator Interaction," ASME Journal of Engineering for Power, 104, pp.729-742, 1982.
5) C. Kato, and M. Ikegawa, "Large Eddy Simulation of Unsteady Turbulent Wake of a Circular Cylinder Using the Finite Element Method," ASME-FED, 117, 49-56, 1991.
6) C. Kato, M. Kaiho, and A. Manabe, "An Overset Finite-

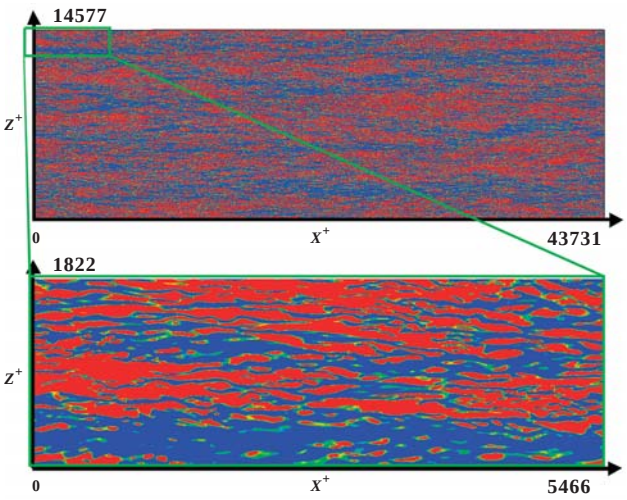

Fig. 7 Plane views of instantaneous near-wall velocity field at $y^+ \sim 11$. Contours of the streamwise velocity fluctuation, blue to red, $u'^+ = -1$ to $u'^+ = 1$. Total computational volume is 43731 and 14577 wall units in the x- and z-directions, respectively.

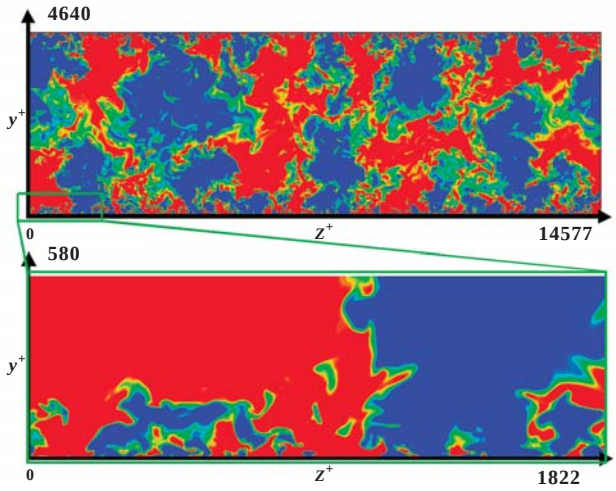

Fig. 8 Cross views of instantaneous velocity field. Contours of the streamwise velocity fluctuation, blue to red, $u'^+ = -1$ to $u'^+ = 1$. Total computational volume is 4640 and 14577 wall units in the y- and z-directions, respectively.

Element Large-Eddy Simulation Method With Application to Turbomachinery and Aeroacoustics," Trans. ASME, 70, pp.32-43, 2003.
7) K. Okita, thesis of Osaka University (in Japanese), 2002.
8) Y. Yamade, et al., "Investigation into noise generation mechanism from a multistage centrifugal pump," Proceeding of 6th Thermal Fluid Engineering Conference, 2005.
9) Y. Yamade, et al., Proceeding of 18th CFD symposium, pp52 (in Japanese), 2004.
10) T. Kawamura, et al., Proceeding of 12th symposium for cavitation, pp109-112 (in Japanese), 2004.
11) N. Kasagi, Y. Sumitani, Y. Suzuki, and O. Iida, "Kinematics of the quasi-coherent vortical structure in near-wall turbulence," Int. J. Heat Fluid Flow, vol. 16, pp.2-10, 1995.
12) J. Kim, P. Moin, and R. D. Moser, "Turbulence statistics in fully developed channel flow at low Reynolds number", J. Fluid Mech., vol.177, pp.133-166, 1987.
13) K. Iwamoto, N. Kasagi, and Y. Suzuki, "Direct numerical simulation of turbulent channel flow at $Re_\tau = 2320$," Proc. 6th Symp. Smart Control of Turbulence, pp.327-333, Tokyo, Japan, Mar. 2005.

ロケットエンジン内部流れのシミュレーション

プロジェクト責任者
古川　正夫　　宇宙航空研究開発機構 総合技術研究本部

著者
清水　太郎　　宇宙航空研究開発機構 総合技術研究本部
山西　伸宏　　宇宙航空研究開発機構 総合技術研究本部
加藤　千幸　　東京大学 生産技術研究所
笠木　伸英　　東京大学大学院 工学系研究科

国産ロケットの信頼性向上及び将来型宇宙輸送システムの開発に資するため、主要エンジン要素(燃焼器系・供給器系)で発生している諸問題(ノズル横力・ターボポンプ内過大圧力振動・燃焼振動)を再現できるCFDコードを開発し、概念設計・システム評価・不具合対策等に使用し、試作・試験のサイクルを短くすることを目標に、プロジェクトを進めた。

本年度は、H-2A 6号機失敗の原因とされるSRB-Aガスリークの非定常計算、ターボポンプ流れ解析用のキャビテーションモデルの基礎検証および高レイノルズ数平行平板間乱流の直接数値計算を実施した。

H-2A 6号機は2003年11月、固体ロケットブースター、SRB-Aの切り離しに失敗した事によりミッションを達成できず、打ち上げ失敗に終わった。この原因として、ノズル内部を流れる高温燃焼ガスによる、ノズルの侵食作用(erosion)により、複合材壁面が破孔し、後部アダプタ内に漏れ出した高温燃焼ガスが、前方ブレス制御用の導爆線を溶解したと推察された。われわれはこれまでに構築した非構造格子法の利点を生かし、後部アダプタ内の形状を忠実に再現、高温燃焼ガス及び壁面加熱率の時間履歴を計測データと比較し、上記シナリオを立証した。最終的にSRB-Aは、高い加熱率を生じる原因ともなった推進薬の表面形状やノズル形状の見直し、及び複合材壁面厚や導爆線位置の見直しを実施した改良形状での地上試験を経て、H-2A 7号機に採用、打ち上げが2005年2月に成功裡に終わった。

ターボポンプの内部流れを定量的に評価できるCFDコードを開発するためには、ターボポンプ内の非定常な流れを精度良く解析し、また内部に発生するキャビテーションの影響を定量的に捉える必要がある。今年度は、遠心ポンプ内部流れの非定常解析に対する精度検証及びキャビテーション流れ解析の基礎検証を行った。この結果良好な結果を得たので、今後は開発したコードをロケットエンジンのインデューサ内部におけるキャビテーション流れに適用し、インデューサ内部に発生するキャビテーションの影響の定量評価を行う。

高レイノルズ数壁乱流で用いることのできる高精度乱流粗視化モデルの構築を目的として、世界最大のレイノルズ数(Re_τ = 2320)平行平板間乱流直接数値シミュレーション(DNS)を行った。従来、実験により確認された高レイノルズ数乱流理論が成立することをDNSで確認した。また、大規模構造はアクティブに乱れを生成し、壁近傍の統計量にも影響を与えるなど、重要で新たな知見を得た。

キーワード: H-2Aロケット，SRB-A，ターボポンプ，LES，高レイノルズ数壁乱流，DNS